

05 DEC. 1979

TRI-PP-79-34  
Sep 1979

CERN LIBRARIES, GENEVA



- 2 -

TRI-PP 79-34 2

Quasi-free scattering of polarized protons†

P. Kitching, C.A. Miller, W.C. Olsen, D.A. Hutcheon,  
W.J. McDonald, and A.W. Stetz††

*University of Alberta, TRIUMF, Edmonton, Alberta, Canada T6G 2E1*

### Abstract

Cross section and polarized asymmetry, energy-sharing spectra have been measured for the  $^{16}\text{O}(\vec{p},2p)$  reaction at an incident energy of 200 MeV for twenty-four different pairs of angles of the detected final state protons. This general survey is intended to test the validity of the distorted wave impulse approximation (DWIA), particularly with respect to the predicted  $j$ -dependent asymmetries caused by the distorting optical potentials and nuclear spin-orbit coupling. Although the data in general confirm this  $j$ -dependence, agreement in detail between DWIA calculations and the asymmetry data tends to become worse as the momentum of the recoiling nucleus increases. Predictably, the cross section calculations show more sensitivity to the optical model parameters than do the asymmetries; within the present limits imposed by scanty elastic scattering data, there seems to remain a choice between predicted  $(p,2p)$  cross sections which either are unreasonably large or have the incorrect energy-sharing shapes. More comprehensive elastic scattering and total reaction cross section data are clearly needed.

(submitted to Nuclear Physics A)

CM-P00067057

1. Introduction

For many years quasi-elastic scattering has been a major source of information concerning proton hole state in nuclei. Both  $(e,e'p)$  and  $(p,2p)$  reactions have been used for this purpose, with the results being interpreted in terms of the distorted wave impulse approximation (DWIA)<sup>1)</sup>. The positions of peaks in the missing energy spectrum are used to determine the energies of the proton hole states, and the shape of the recoil momentum distribution gives information on the angular momentum of the hole state. More recently, Jacob *et al.*<sup>2)</sup> have suggested using the effects of distortion to extract additional information concerning the  $j$ -value of the hole state. These authors predicted that if a measurement of the  $(p,2p)$  reaction were made when one of the detected protons has a lower energy than the other, then for an appropriate direction of the recoil momentum one can preferentially select an orbital angular momentum projection for the knocked out proton. Because of spin-orbit coupling, the target protons in the nucleus are thereby effectively polarized by a combination of distortion and kinematic effects, and the value of this effective polarization is dependent on the  $j$ -value of the target proton. When polarized incident protons are used the cross section is sensitive to the relative directions of the polarizations of the incident and target protons. Hence,  $j$ -dependent asymmetries in the  $(p,2p)$  cross section are predicted. Such asymmetries have been observed in an earlier experiment<sup>3)</sup> at TRIUMF to depend on known  $j$ -values of the struck proton in the predicted way, suggesting that this effect may be used as a tool for studying the  $j$ -values of proton hole states.

The other major reason for interest in  $(\vec{p},2p)$  asymmetry measurements is that they are expected to afford a more stringent test of reaction models than cross sections. Questions such as the validity of the factorization approximation and the importance of spin-orbit distortions may be addressed more easily, both because the observed effects must be entirely due to distortions and because parameter sensitivities are less of a problem. Off-shell effects might be studied more easily since the  $A_{yy}$  spin-spin correlation term entering into the observed  $j$ -dependent asymmetry is a stronger function of energy than cross sections are.

In an attempt to shed light on some of these questions we have performed a comprehensive series of measurements of both cross sections and

† Work supported in part by the Natural Sciences and Engineering Research Council of Canada.

†† Present address: Department of Physics, Oregon State University, Corvallis, Oregon, U.S.A. 97331.

experimental cross sections (for energy bins of 20 MeV)

$$\frac{d^5\sigma}{d\Omega_1 d\Omega_2 d(E_1-E_2)} \quad (1)$$

were calculated. In these calculations correction factors were applied for:

- (a) missing wire chamber co-ordinates
- (b) discarded multiple hits in MWPC co-ordinates
- (c) pile-up in NaI (T<sub>L</sub>) detectors
- (d) dead time of the data collection system
- (e) NaI (T<sub>L</sub>) detector efficiencies

The major contributor to the dead time, that of the computer itself, was measured by comparing the number of events accepted by the computer with the number presented. The overall dead time of the system was monitored by means of a pulser system which flashed light-emitting diodes attached to all of the plastic scintillators and NaI (T<sub>L</sub>) detectors, and also pulsed one wire of each sense plane of the MWPC's. The fraction of these pulses that was not recorded by the computer as a valid event was a direct measurement of the dead time of the overall system, which was usually about 20%. Pulse events were labelled on the tape by setting a bit in the pattern register.

Cross sections were calculated in this way for each set of boom angles and for each run. In general the value of the polarization (P) of the incident beam varied from run to run. All runs for a given setting of the boom angles were fitted by the least squares method with a straight line of the form:

$$\frac{d^5\sigma}{d\Omega_1 d\Omega_2 d(E_1-E_2)} = \left( \frac{d^5\sigma}{d\Omega_1 d\Omega_2 d(E_1-E_2)} \right)_0 \times (1 + AP),$$

where  $\left( \frac{d^5\sigma}{d\Omega_1 d\Omega_2 d(E_1-E_2)} \right)_0$  is the unpolarized cross section and A is the asymmetry. Thus the  ${}^0_{16}O(p,2p)$  unpolarized cross sections and asymmetries were obtained as a function of (E<sub>1</sub>-E<sub>2</sub>) for each setting of the boom angles and for protons ejected from both the P<sub>3/2</sub> and P<sub>1/2</sub> states. The overall resolution in recoil momentum was typically <30 MeV/c, with the major contributions arising from the finite bin size in (E<sub>1</sub>-E<sub>2</sub>) and the solid angle sizes.

### 5. Results and conclusion

The measured asymmetries and cross sections are shown in figs. 4 through 27. The errors shown are statistical only; where they are not visible, they are smaller than the data points. In the case of the asymmetries, the systematic error is estimated to be ±5% arising mainly from uncertainty in the polarization of the incident beam and from uncertainty as to where to cut the missing energy spectrum (energy resolution effect). For the cross section, the systematic error is in the calibration of the ion chamber (±5%), the thickness of the target (±5%), the solid angles subtended by the detectors (±3%), the NaI efficiencies (±3%), and the finite energy resolution effects (±5%). For symmetric angle pairs, the data on either side of the point of equal final state proton energies must be redundant (with asymmetries inverted) but they were not averaged so that this degree of internal consistency of the data can be seen. The curves shown on the figures are the results of factorized DWIA calculations<sup>1</sup>) in which the cross section is given by

$$\frac{d^3\sigma}{d\Omega_1 d\Omega_2 d(E_1-E_2)} = C^2 S K \sigma_{pp} \sum_m |T_L^m|^2, \quad (2)$$

where C<sup>2</sup>S is the spectroscopic factor for the experimentally chosen residual nuclear state, K is a kinematic and phase space factor, and σ<sub>pp</sub> is the half-off-shell p-p cross section<sup>4</sup>). The transition amplitudes T<sub>L</sub><sup>m</sup> are calculated<sup>7</sup>) using

$$T_L^m = (2L+1)^{-1/2} \int d^3\vec{r} \chi_1^{(-)*}(\vec{r}) \chi_2^{(-)*}(\vec{r}) \psi_L^m(\vec{r}) \chi_0^{(+)}(\vec{r}), \quad (3)$$

where the χ's are optical model scattering wave functions and ψ<sub>L</sub><sup>m</sup> is the initial bound state wave function of the struck proton with orbital angular momentum L. ψ<sub>L</sub><sup>m</sup> is calculated in a Saxon-Woods potential including a spin-orbit term with parameters derived from elastic scattering data by Elton and Swift<sup>8</sup>). The spin-orbit part of the optical model potentials has been neglected. Recent calculations including the spin-orbit potential have indicated that for knockout from the p-shells of <sup>16</sup>O the effects are of the order of 10-15% [ref. 9)].

In calculating σ<sub>pp</sub>, the polarization, P<sub>0</sub>, of the incident beam and the effective initial polarization, P<sub>s</sub>, of the struck proton are taken into account in the present simplified co-planar case using

$$\sigma_{pp} = \sigma_0 (1 + (P_0 + P_S) \cdot A_y + P_0 \cdot P_S A_{yy}) \quad (4)$$

where  $\sigma_0$  is the unpolarized cross section,  $A_y$  is the p-p analyzing power and  $A_{yy}$  is the spin-correlation parameter (often called  $C_{nn}$ ).  $P_S$  is determined by the  $T_{LL}^m$ 's:

$$P_S = \frac{\sum_m (c_L^m(+)) - c_L^m(-)}{\sum_m (c_L^m(+)) + c_L^m(-)} \frac{|T_{LL}^m|^2}{|T_{LL}^m|^2} \quad (5)$$

where the  $C_L^m$ 's are combinations of Clebsch-Gordon coefficients reflecting the spin-orbit coupling of the struck proton and the coupling of the resultant  $j$  to that of the residual nucleus.  $P_S$  can be non-zero only if  $L$  is non-zero, and the experiment is non-symmetric with respect to the kinematic attributes of the final state protons. If such is the case, it is  $j$ -dependent in general. As can be shown from eq. (4), only  $A_{yy}$  and not  $A_y$  contributes to the experimental determination of  $P_S$  by measuring asymmetries (i.e. changing the sign of  $P_0$ ).

The three required p-p observables,  $\sigma_0$ ,  $A_y$  and  $A_{yy}$  are off-shell quantities. Provided that the direct effects of the distorting potentials on the p-p interaction can be neglected, the observables may be calculated using the half-shell prescription which accounts only for the binding energy and momentum mismatch. In most previous analyses, an on-shell extrapolation has been used in which the energy at which the observables are evaluated corresponds to the relative energy of the two protons in the initial state (ISP) or final state (FSP) or some average of the two. If only cross sections are required (which do not vary rapidly with energy) the consequent ambiguity is usually not serious. Because  $A_y$  and  $A_{yy}$  are more strongly energy dependent, the present calculations use the half-shell prescription (HSP) in which off-shell information is obtained from a convenient phenomenological nucleon-nucleon potential. A factorized t-matrix method<sup>10</sup> for calculating half-off-shell amplitudes is used which incorporates on-shell information from experimentally determined phase shifts<sup>6</sup> with off-shell information from a potential model. Such calculations comparing (p,2p) cross sections and asymmetries using two very different potential models in kinematic situations where off-shell effects are expected to be much more important than in the present experiment have indicated a lack of sensitivity to the choice of potential model<sup>11</sup>). Therefore it seems likely that the

separable non-local potential of Mongan<sup>12</sup>) used here will be more than adequate to account for the relatively mild off-shell effects expected for the present data. Parenthetically we note here that neither the ISP or FSP is consistently closer to the HSP results; it depends on the kinematic situation and on whether one is considering cross sections or asymmetries.

The optical potential used to generate the distorted waves is of standard Woods-Saxon form with parameters taken from a systematic fit to intermediate energy elastic scattering data on <sup>12</sup>C [ref. 13)]. The resulting parameter set including no surface imaginary part was found to fit acceptably some <sup>16</sup>O elastic scattering data and yield reasonable values for the total reaction cross section ( $\sigma_R$ ). However, the scarcity in the required energy region of both data and attempts at systematic energy-dependent fits mean that the optical potentials are probably the weakest aspect of the current DWIA calculations. Future efforts to fit new intermediate energy elastic scattering data might do well to be guided by the optical potential predictions of nuclear matter calculations<sup>14</sup>). This may help to ameliorate the problem that asymptotic information such as elastic scattering data does not unambiguously define the wave function and potential inside the nucleus.

In comparing these DWIA calculations with the data, we note that in general asymmetries show the expected  $j$ -dependence. This can be taken to be a more significant success for the DWIA than tests involving only cross sections, both because these asymmetries are entirely due to the effects of distortions and because, somewhat paradoxically, parameter studies have shown that asymmetries are less sensitive than cross sections to the choice of bound state and optical model potential parameters<sup>2</sup>). It certainly appears that this technique would aid in identifying unknown  $j$ -values of hole states. However, the degree of agreement with the data varies from angle to angle. At symmetric angles with asymmetric energy-sharing, the agreement is significantly better than at asymmetric angles. In such tests of the reaction model, it is clearly important that data be taken in a wide range of kinematic conditions.

The cross section data are less well fitted by the calculations, both in regard to the energy-sharing shapes and the fact that values of  $C_{2S}$  of

0.7 times the simple shell model expectations (2 for the  $P_{1/2}$  state and 4 for the  $P_{3/2}$ ) are required to normalize the calculations downward to the data. The reason this result is in apparent conflict with better fits for the preliminary data previously reported<sup>3</sup>) is that those calculations were done with an optical parameter set which was later found to yield total reaction cross sections much too large for  $^{16}\text{O}$ ; by a factor of 2 at 100 MeV, for example. Although that more absorptive potential affects the  $(p,2p)$  cross sections much more than asymmetries, it does result in somewhat larger asymmetries which are more consistent with the data at angle pairs such as  $30^\circ$ - $30^\circ$  where the values are typically large. Therefore, both asymmetries and cross sections seem to be suggesting that somehow stronger effective absorption is required in the calculations.

There is one area of marked disagreement between the calculated and measured cross sections that probably has a ready explanation. As both detector angles increase beyond  $60^\circ$  and consequently the recoil momentum surpasses  $1 \text{ fm}^{-1}$ , the cross-section data falls much less rapidly than the calculated values. In view of predictions of high momentum components in the nuclear overlap integral not accounted for in the single particle wave function, this is not unexpected. Zabolitzky and Ey<sup>15</sup>), for example, have shown that nucleon-nucleon correlations can have a very significant effect above  $1 \text{ fm}^{-1}$ . However, one must beware of the temptation to compare their momentum distributions directly with the data because of the "momentum smearing" effect of distortions; a steeply falling distribution will be effectively sampled at a smaller momentum than that of the recoil.

In the face of the generally disappointing fits to the cross sections, it is natural to ask whether there are adjustments to the optical parameters which would maintain reasonable accord with elastic and  $\sigma_R$  data while improving agreement with  $(p,2p)$  data. While we have not investigated this problem exhaustively, we have done calculations using potentials with a larger imaginary radius derived by imposing a smooth energy dependence on the parameters for  $^{16}\text{O}$  and  $^{12}\text{C}$  resulting from previous fits by various groups at different energies<sup>16</sup>). Above 70 MeV, this required some adjustment of the parameters for the imaginary potential in a manner which approximately "conserved"  $\sigma_R$ . In table 1, the resulting set (set B) for these representative energies is compared to that of Abdul-Jalil and Jackson (set A). Both sets yield values of  $\sigma_R$  that are

reasonable below 150 MeV but somewhat small at 200 MeV. DWIA calculations using set B are compared with a selected subset of the  $(p,2p)$  data in fig. 28. The magnitude of the cross sections is fitted even less well than for parameter set A; a value of 0.5 times the simple shell model values is required for  $^{12}\text{C}$ . Although the shapes of the cross sections are in somewhat better agreement, the predicted asymmetries are too small at  $30^\circ$ - $30^\circ$ . There is little change to the shapes of the asymmetries at angle pairs where they were not well fitted. Therefore, it seems unlikely that inadequacies in the optical potentials can entirely account for the present discrepancies between the DWIA and the data.

The other important input to the calculation is the single particle wave function used to approximate the nuclear overlap integral representing the initial bound state. The shape and especially the magnitude of the  $(p,2p)$  cross section is sensitive to the rms radius of this wave function, although the asymmetries, in contrast, are very insensitive. However, since the Elton and Swift wave function used here is consistent with elastic electron scattering and their wave functions for  $^{12}\text{C}$  and other nuclei seem to fit  $(e,e'p)$  data quite well<sup>17</sup>), there seems to be little justification for attempting to adjust the parameters. In any case, such adjustment appears to be ineffectual in improving the overall fit to the  $(p,2p)$  cross sections. If the p-shell particle-to-core rms radius is increased from the Elton and Swift value of 2.86 fm to 3.2 fm in order to better fit the energy-sharing shapes, then  $^{12}\text{C}$ 's is required to fall to 0.5 times the shell model expectation.

There is one relatively simple phenomenon which may be relevant to this situation. Nuclear matter calculations indicate that the non-locality of the optical potential is even larger than that required to account for the energy dependence of the asymptotically equivalent local potential. (At lower energies the intrinsic energy dependence of the non-local potential has the opposite sign and has a cancelling effect.) The asymptotically equivalent local potential which we are presumably using is not equivalent with regard to the wave function inside the nucleus. It has been noticed by Perry and Buck<sup>18</sup>) that wave functions calculated from a non-local potential have amplitudes reduced inside the potential compared with those calculated from the equivalent local potential. The DWIA calculation involves a product of the three scattering

wave functions which is then squared to yield the distorted momentum distribution so that such effects are amplified by the sixth power. A crude attempt to determine the importance of this effect was made by multiplying the scattering wave function amplitudes by the nuclear density-dependent factor  $\left\{\frac{m}{m_0}\right\}^{1/2}$ , values for which were taken from nuclear matter calculations<sup>19</sup>).  $m$  is an effective mass which characterizes the non-locality of the potential. The radial dependence of the nuclear density was taken to be that suggested by Negele, also given in ref. 19). Including this effect reduces the calculated (p,2p) cross sections by a factor ranging from 1.2 at the more forward angle pairs to 2.0 at 65°-65°. Although energy-sharing cross-section shapes are little improved and asymmetries are very little affected, it appears to be important to include this effect in DWIA calculations, preferably in a more self-consistent manner than here.

In summary, DWIA calculations using the set A optical parameters, Elton-Swift bound state wave function, and accounting crudely for the effects of the non-locality of the optical potentials yield reasonable spectroscopic factors for both  $P_{1/2}$  and  $P_{3/2}$  hole states. As well, the predicted j-dependence of the asymmetries is confirmed by the data. However, the angle and energy-sharing dependence of the cross sections and, in some cases, the asymmetry shapes are not well described by the calculations. One possible reason for this problem is lack of knowledge of the optical potential. It is also possible that some of the discrepancies arise from coupling terms of order  $\frac{1}{A}$  omitted from the three-body Schrödinger equation. In addition, two-step processes may become important contributors, especially at high recoil momenta. Some recent calculations<sup>23</sup>) suggest, however, that at 200 MeV such effects are small (<10% of the observed cross section). Yet another, more interesting explanation is failure of the approximation made in factorizing the matrix element. There has been recent experimental and theoretical work investigating this question at intermediate energy. Some <sup>40</sup>Ca(p,2p) measurements<sup>20</sup>) at 148 MeV using an experimental geometry chosen specifically for this purpose have yielded results consistent with the factorized DWIA. However, it is worth noting that D(p,2p) measurements at 50 MeV yielded essentially the same flat quasi-free angular correlation whereas it is now known that this is fortuitous and that only full three-body calculations can adequately deal with the D(p,2p) and D(p,pn) reactions at that

energy<sup>21</sup>). In the area of theoretical investigations, Koshel has compared with the corresponding factorized results the predictions of unfactorized ("finite range") calculations using a pseudo-potential for the p-p interaction<sup>22</sup>). He has found significant discrepancies in some kinematic situations, even at an energy as high as 200 MeV. Therefore, this question appears to remain an open one and further theoretical work is needed.

#### References

- 1) G. Jacob and Th.A.J. Maris, Rev. Mod. Phys. 45 (1973) 6, and Rev. Mod. Phys. 38 (1966) 121.
- 2) G. Jacob, Th.A.J. Maris, C. Schneider, and M.R. Teodoro, Nucl. Phys. A257 (1976) 517.
- 3) P. Kitching, C.A. Miller, D.A. Hutcheon, A.N. James, W.J. McDonald, J.M. Cameron, W.C. Olsen, and G. Roy, Phys. Rev. Lett. 37 (1976) 1600.
- 4) E.F. Redish, G.J. Stephenson, Jr., and G.M. Lerner, Phys. Rev. C2 (1970) 1665.
- 5) J.M. Cameron, P. Kitching, R.H. McAmis, C.A. Miller, G.A. Moss, J.G. Rogers, G. Roy, A.W. Stetz, C.A. Goulding, and W.T.H. van Oers, Nucl. Instr. and Meth. 143 (1977) 399.
- 6) R.A. Arndt, R.H. Hackman, and L.D. Roper, Phys. Rev. C15 (1977) 1002.
- 7) D.F. Jackson and T. Berggren, Nucl. Phys. 62 (1965) 353.
- 8) L.R.B. Elton and A. Swift, Nucl. Phys. A94 (1967) 52.
- 9) N.S. Chant, P. Kitching, P. G. Roos, and L. Antonuk, Phys. Rev. Lett. 43 (1979) 495.
- 10) T.R. Mongan, Phys. Rev. 184 (1969) 1888.
- 11) C.A. Miller and A.W. Thomas, to be published; C.A. Miller, *Proc. of the Advanced Study Institute on Common Problems in Low and Medium Energy Physics*, Banff (1978).
- 12) T.R. Mongan, Phys. Rev. 178 (1969) 1597.
- 13) I. Abdul-Jalil and D.F. Jackson, abstract #AC21 of Contributed Papers of the Eighth International Conference on High Energy Physics and Nuclear Structure, Vancouver, 1979, p.99.
- 14) J.-P. Jeukenne, A. Lejeune, and C. Mahaux, Phys. Rep. 25C (1976) 85.
- 15) J.G. Zabolitzky and W. Ey, Phys. Lett. 76B (1978) 527.
- 16) W.T.H. van Oers and J.M. Cameron, Phys. Rev. 184 (1969) 1061; V. Comparat, R. Frascaria, N. Marty, M. Morlet, and A. Willis, Nucl. Phys. A221 (1974) 403; W.T.H. van Oers, private communication.
- 17) J. Mougey, M. Bernheim, A. Bussière, A. Gillebert, Phan. Xuan Hô, M. Priou, D. Royer, I. Sick, and G.J. Wagner, Nucl. Phys. A262 (1976) 461;
- 18) J. Mougey, Bull. Am. Phys. Soc. 23 (1978) 535.
- 19) F.G. Perey, Phys. Rev. 131 (1963) 745; F.G. Perey and B. Buck, Nucl. Phys. 32 (1962) 353.
- 20) J.-P. Jeukenne, A. Lejeune, and C. Mahaux, Phys. Rev. C16 (1977) 80.
- 21) P.G. Roos, N.S. Chant, D.W. Devins, D.L. Friesel, W.P. Jones, A.C. Attard, R.S. Henderson, I.D. Svalbe, B.M. Spicer, V.C. Officer, and G.G. Shute, Phys. Rev. Lett. 40 (1978) 1439.
- 22) E.L. Peterson, R.G. Alias, R.O. Bondelid, D.I. Bonbright, A.G. Pieper, and R.B. Theus, Phys. Rev. Lett. 27 (1971) 1454.

- 22) R.D. Koshel, private communication.  
 23) Y. Kudo and J. Mano, preprint, Osaka City University (1979).

Table 1

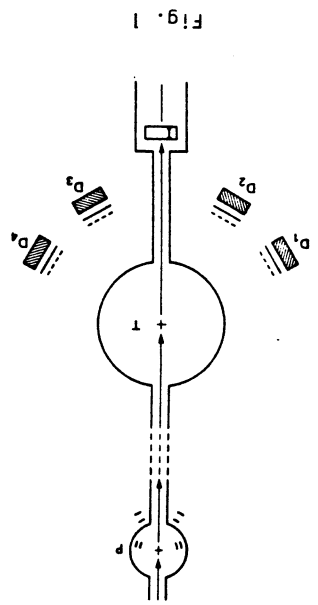
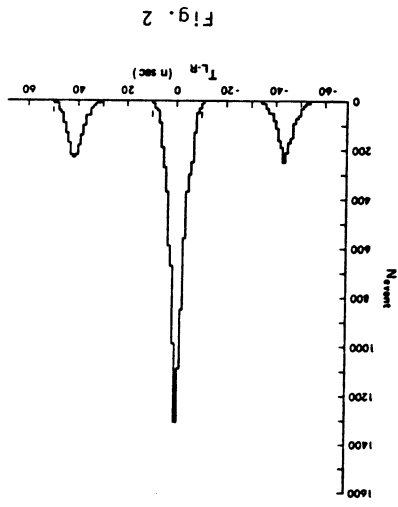
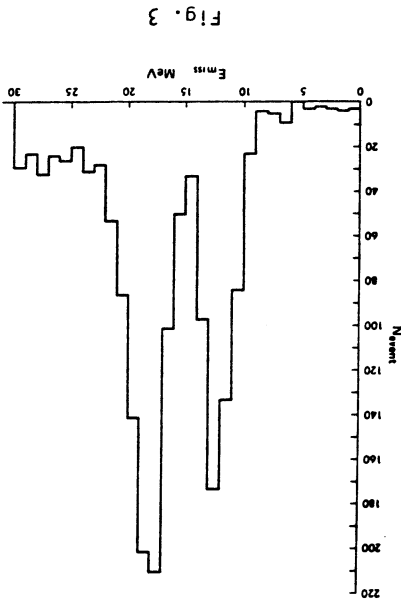
Optical model parameters for set A (set B) and the corresponding total reaction cross sections for protons on $^{16}\text{O}$		50	100	200
Energy (MeV)		50	100	200
$V_0$ (fm)	1.45 (1.14)	1.45 (1.29)	1.45 (1.45)	
$a_0$ (fm)	0.554 (0.70)	0.554 (0.576)	0.554 (0.454)	
$V$ (MeV)	21.7 (54)	16.2 (22)	8.3 (4.6)	
$r_i$ (fm)	0.932 (1.3)	0.932 (1.3)	0.932 (1.3)	
$a_i$ (fm)	0.612 (0.6)	0.612 (0.6)	0.612 (0.6)	
$W_D$ (MeV)	27 (3.95)	27 (9.3)	27 (10)	
$W_S$ (MeV)	0 (2.45)	0 (0)	9 (0)	
$\sigma_R$ (mb)	401 (417)	307 (294)	236 (214)	

Figure Captions

1. Schematic diagram showing the experimental arrangement of target and counters.
2. A typical event defining time-of-flight spectrum showing the time difference between particles passing through the left and right plastic detectors of a given pair of counter telescopes.
3. A typical "missing energy" spectrum showing two peaks corresponding to the knock-out of  $P_{1/2}$  and  $P_{3/2}$  protons from  $^{16}\text{O}$ .

4-27 inclusive: Plots of the measured asymmetries and cross sections for all angle combinations set in the experiment, together with curves representing DWIA calculations using parameter set A (see table 1) as described in the text. The abscissa is the kinetic energy of one of the final state protons, and the ordinate is the cross section as defined by expression (1) in the text.

28. A composite drawing showing results for selected angle pairs and the DWIA curves using parameter set B (see table 1).



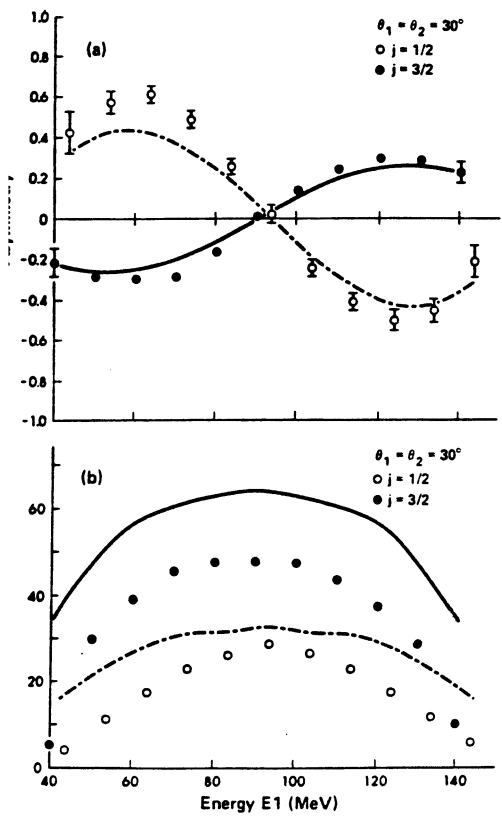


Fig. 4

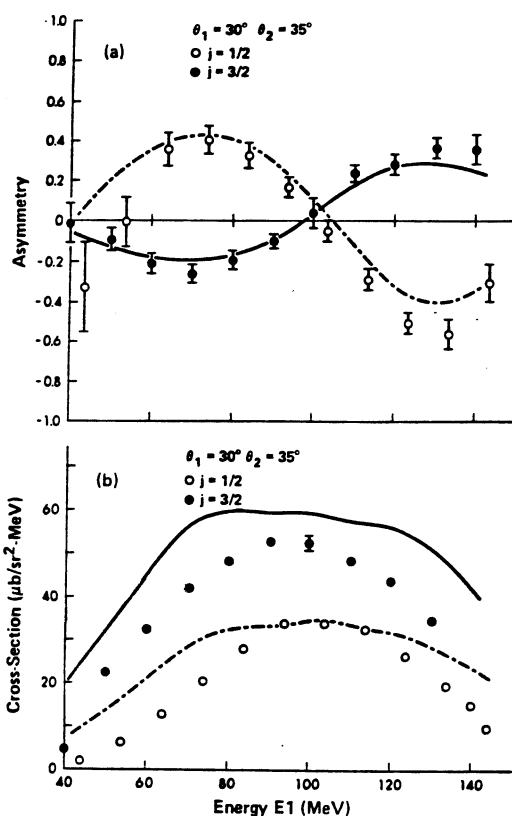


Fig. 5

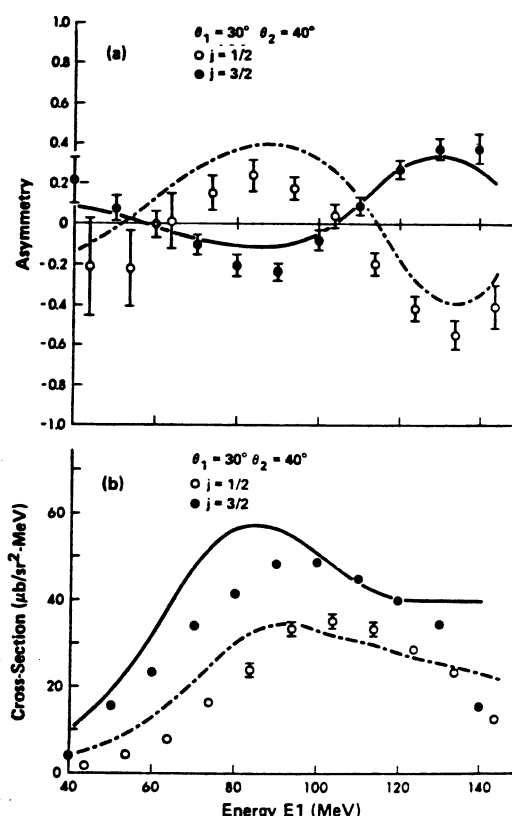


Fig. 6

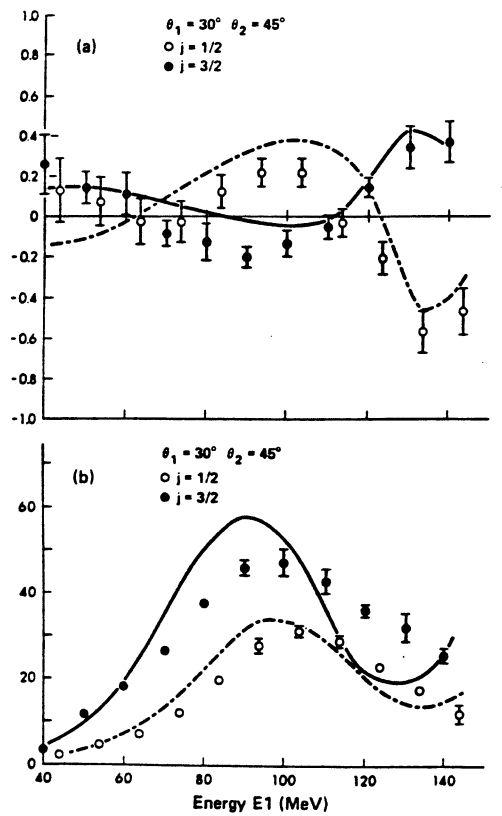


Fig. 7

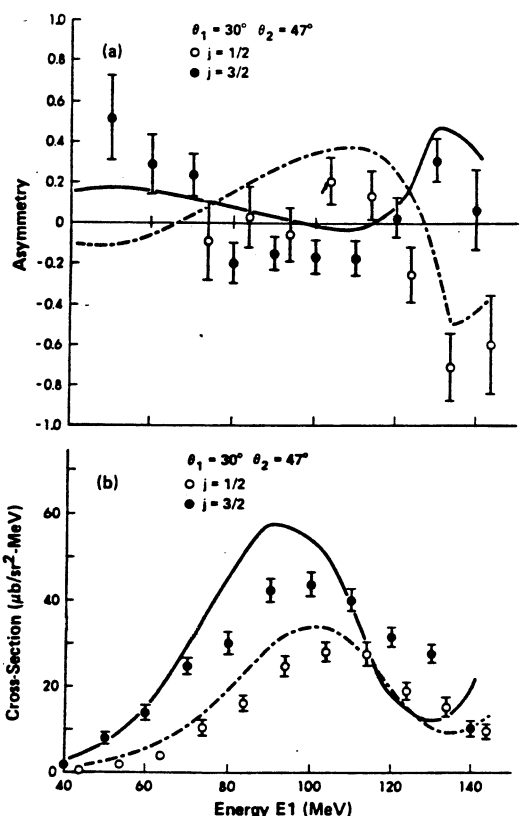


Fig. 8

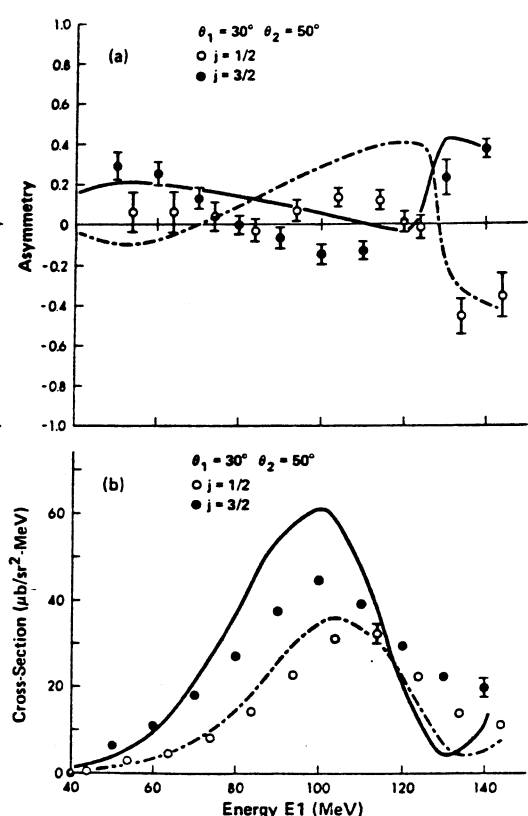
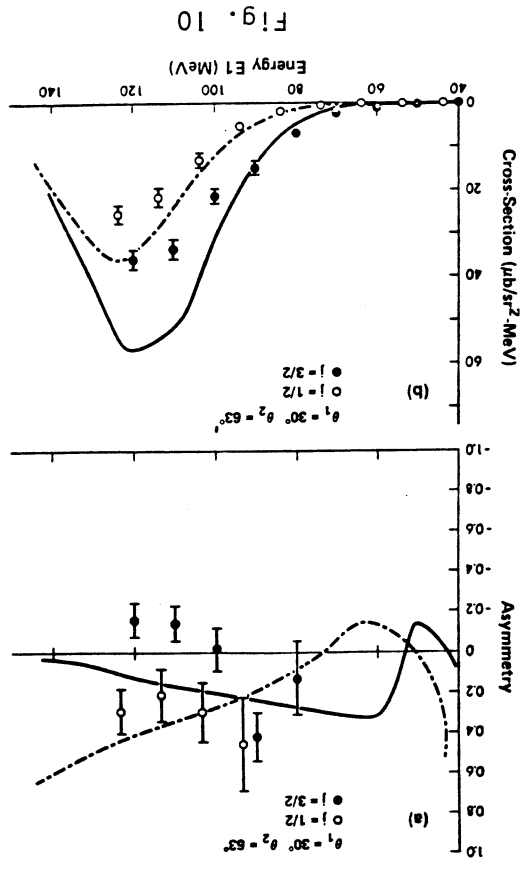
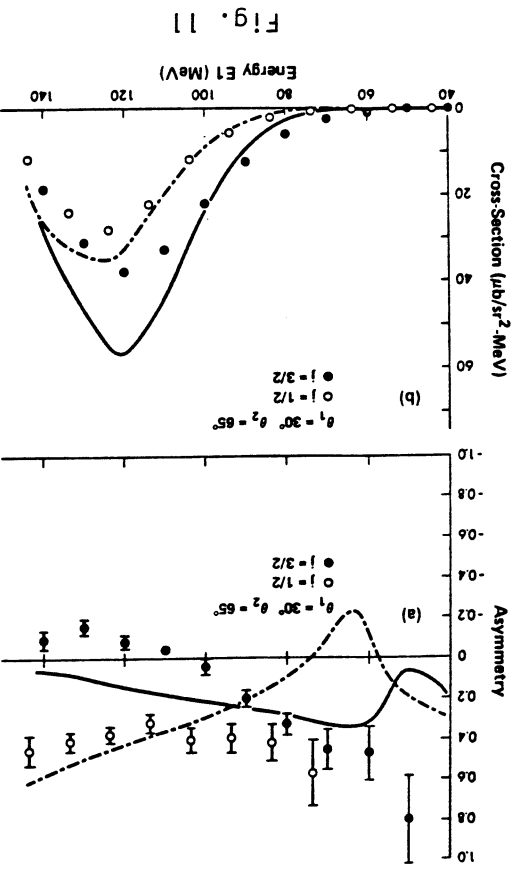
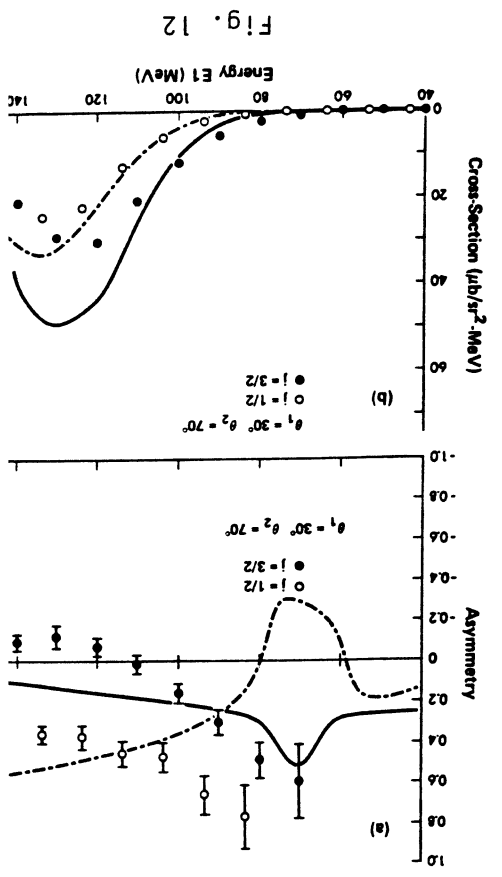
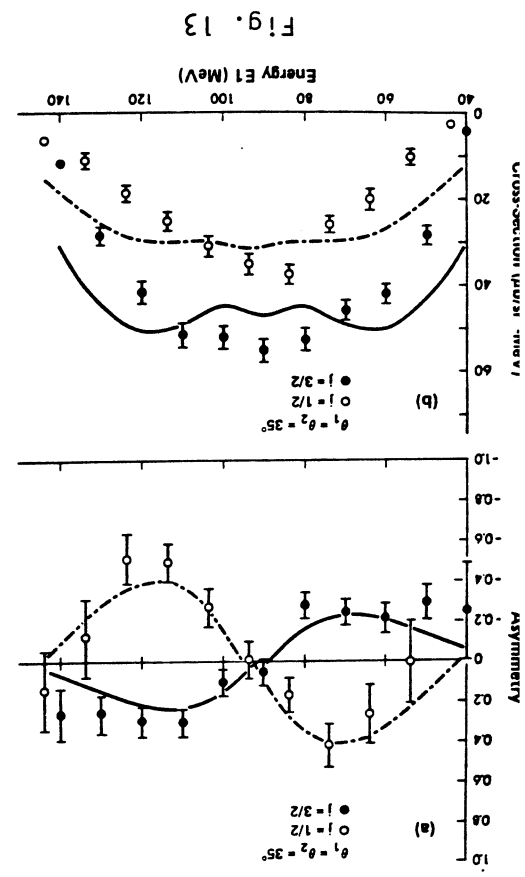
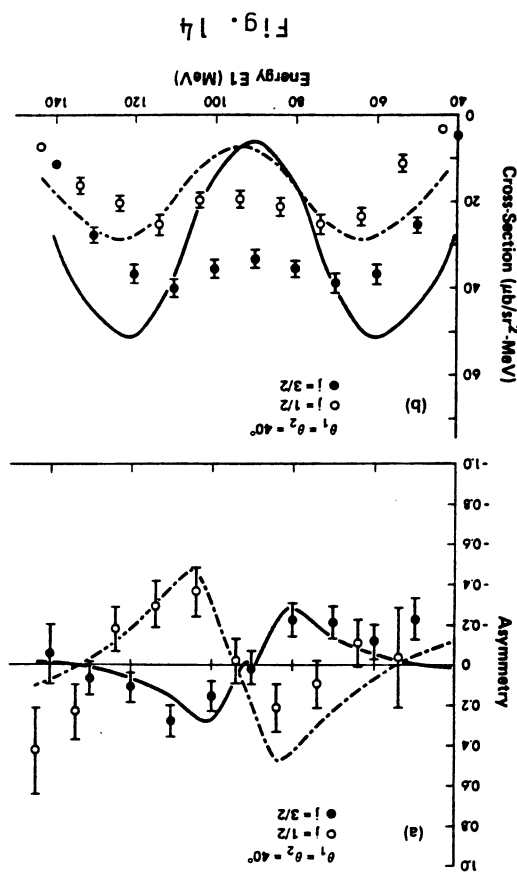
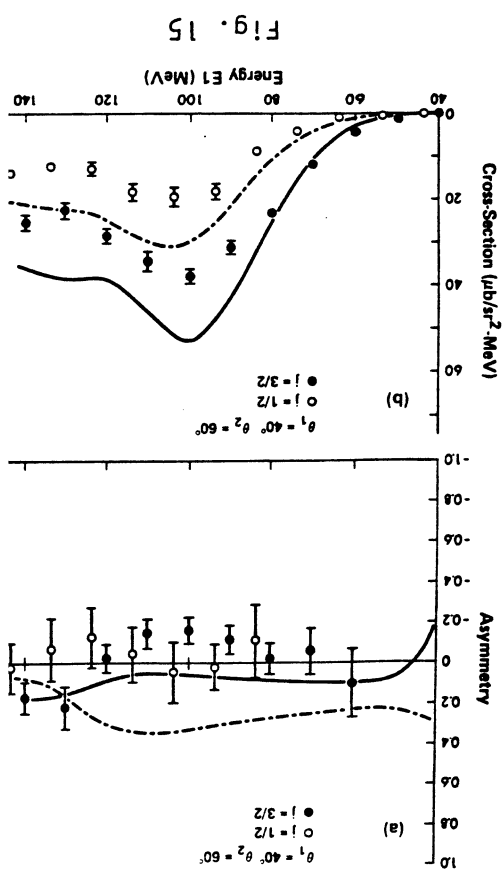


Fig. 9





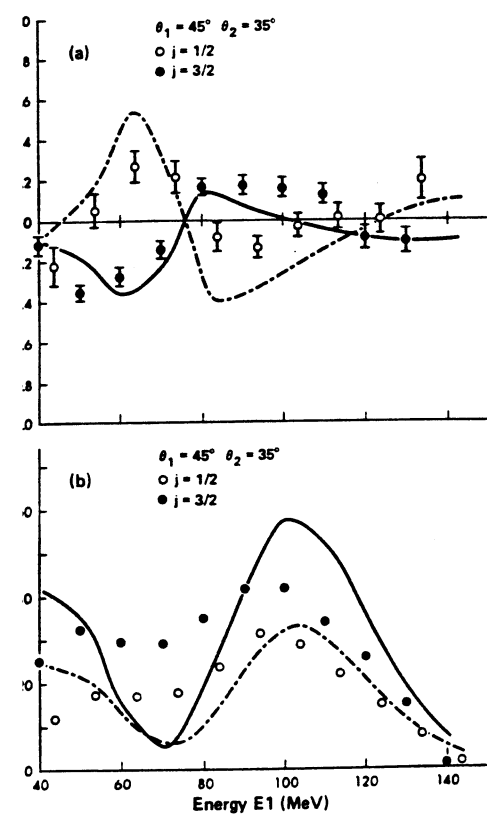


Fig. 16

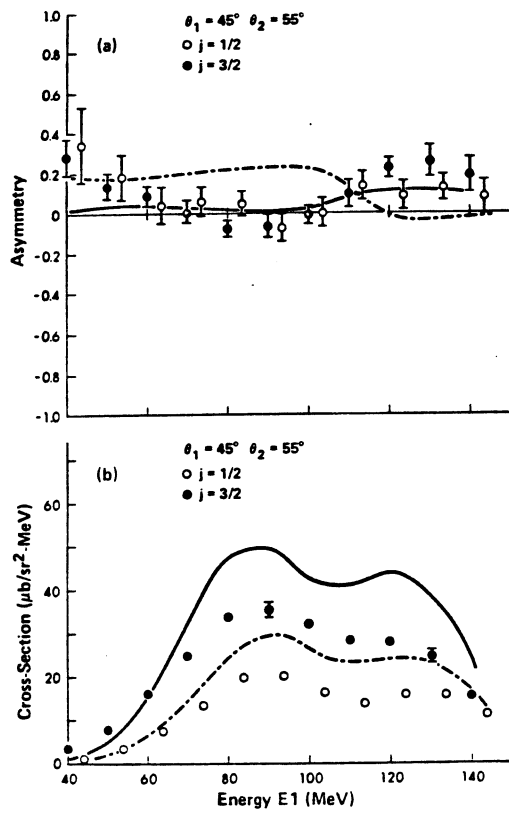


Fig. 17

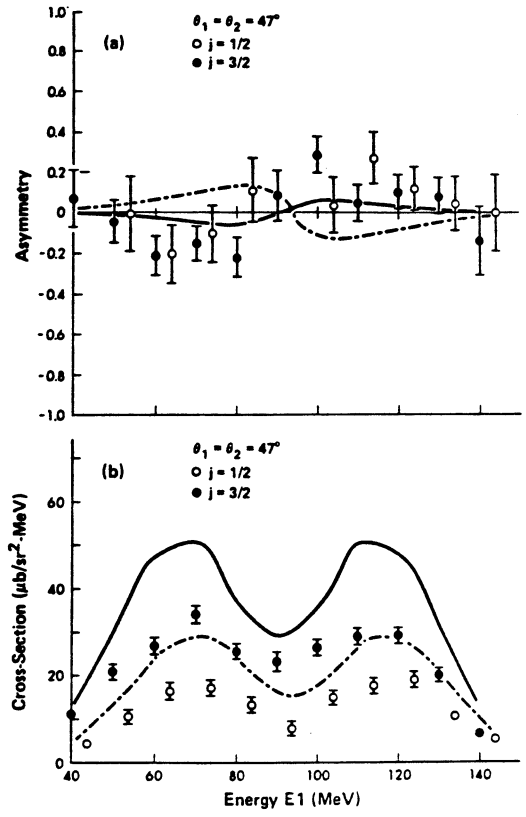


Fig. 18

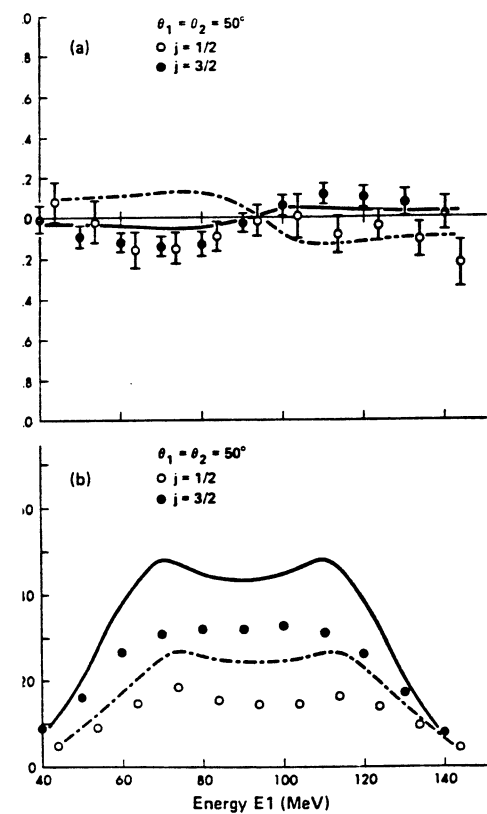


Fig. 19

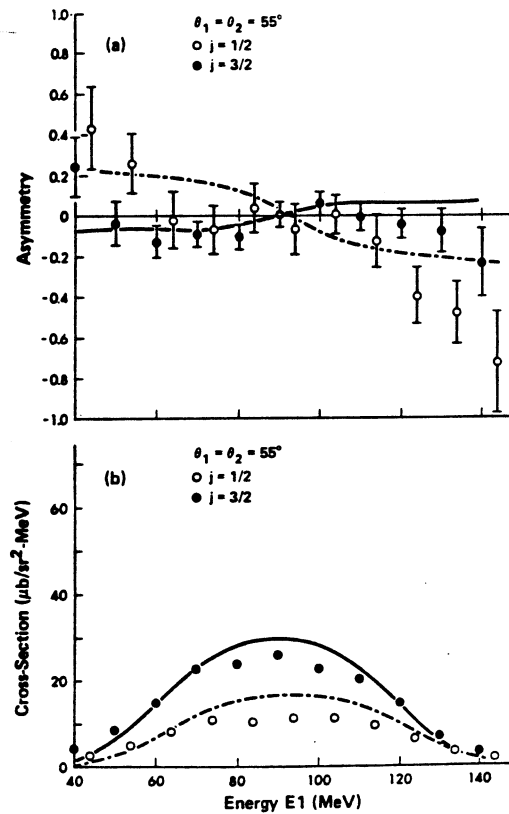


Fig. 20

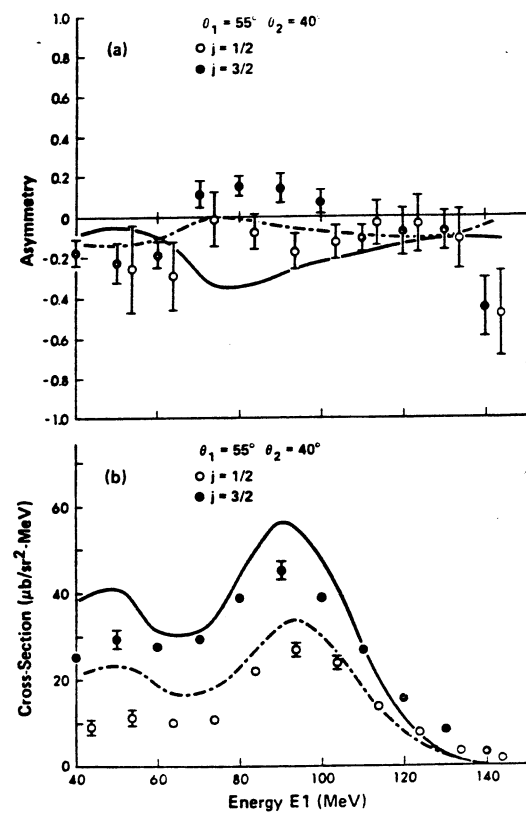


Fig. 21

Fig. 25

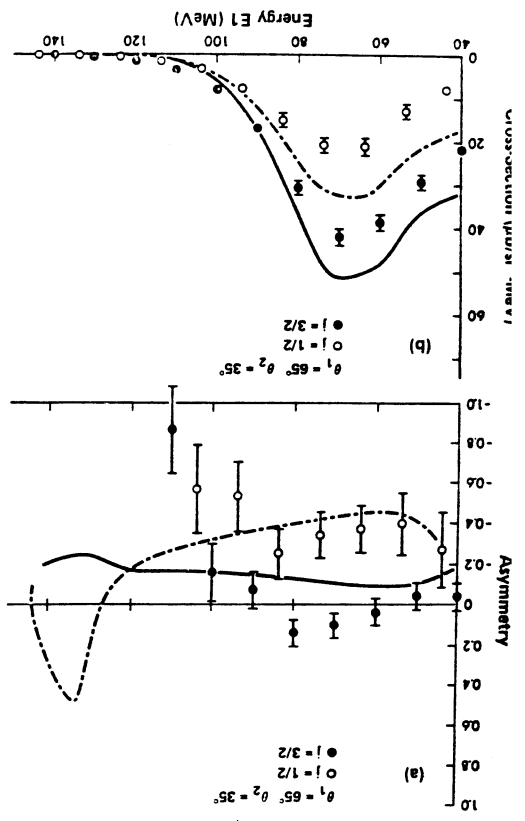


Fig. 26

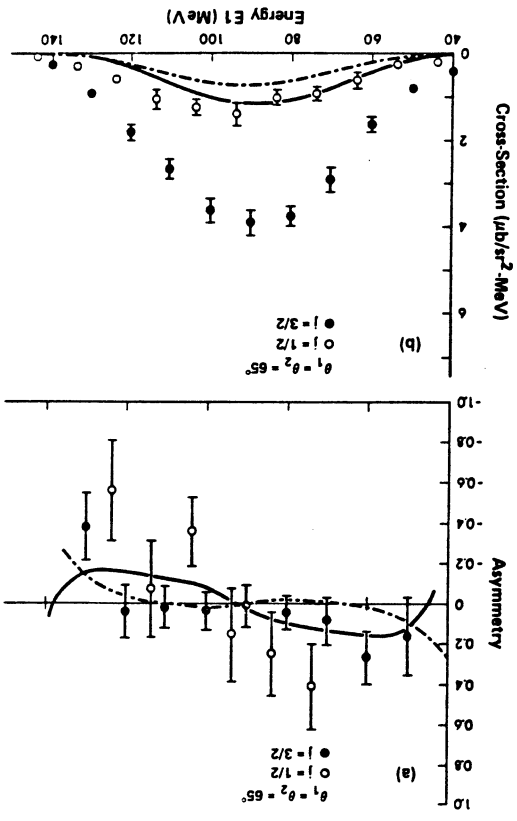


Fig. 27

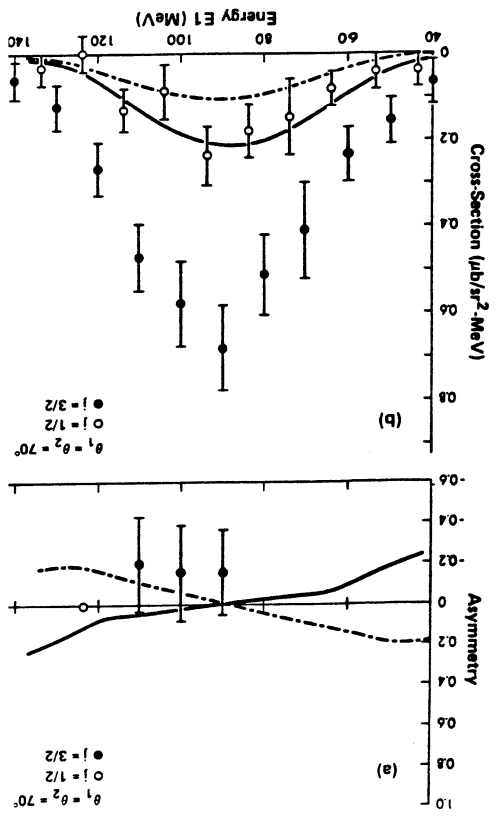


Fig. 22

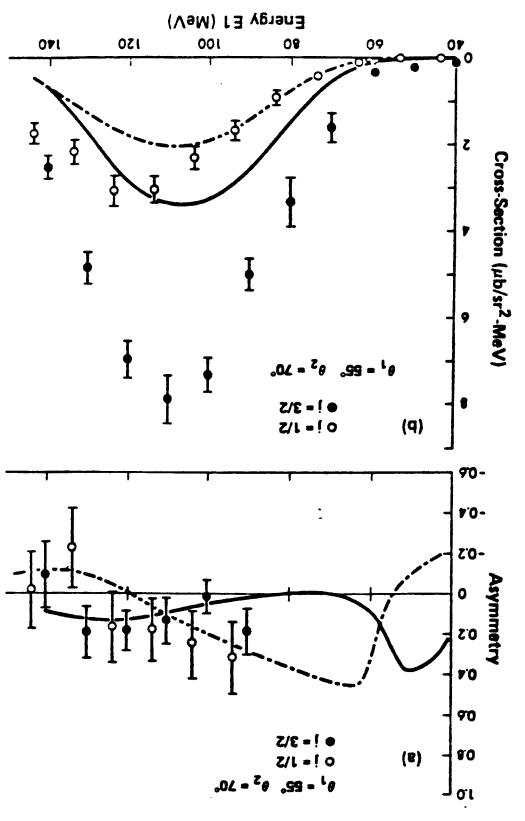


Fig. 23

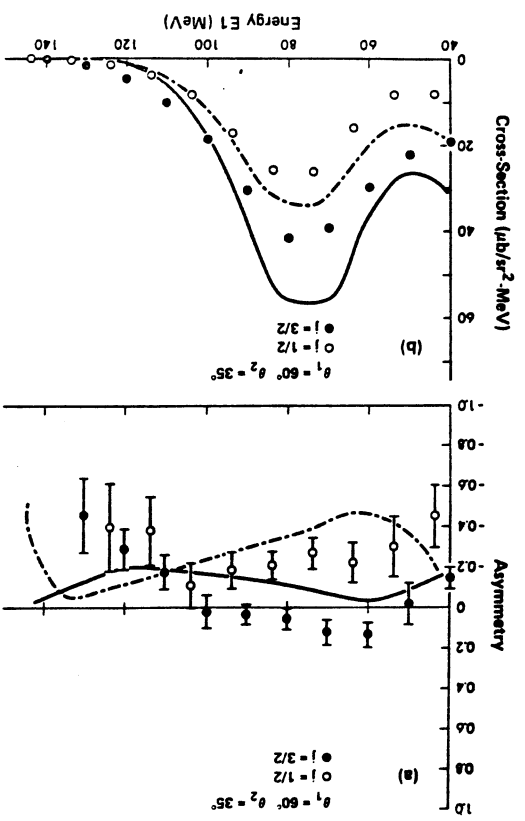
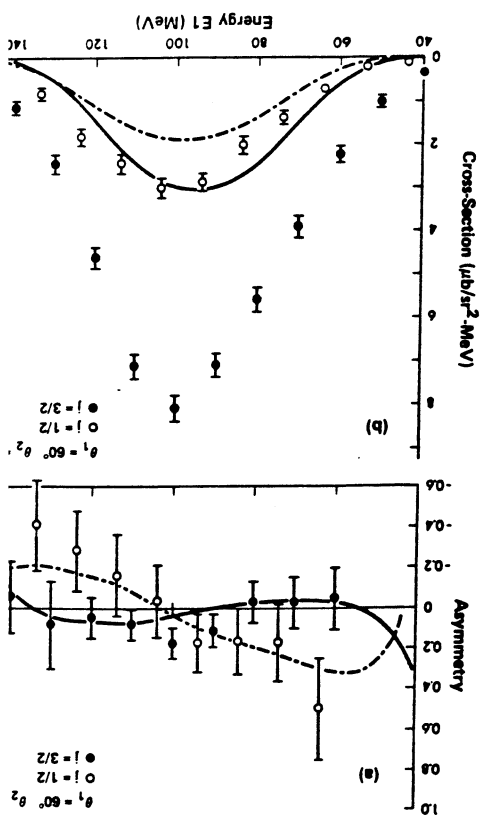


Fig. 24



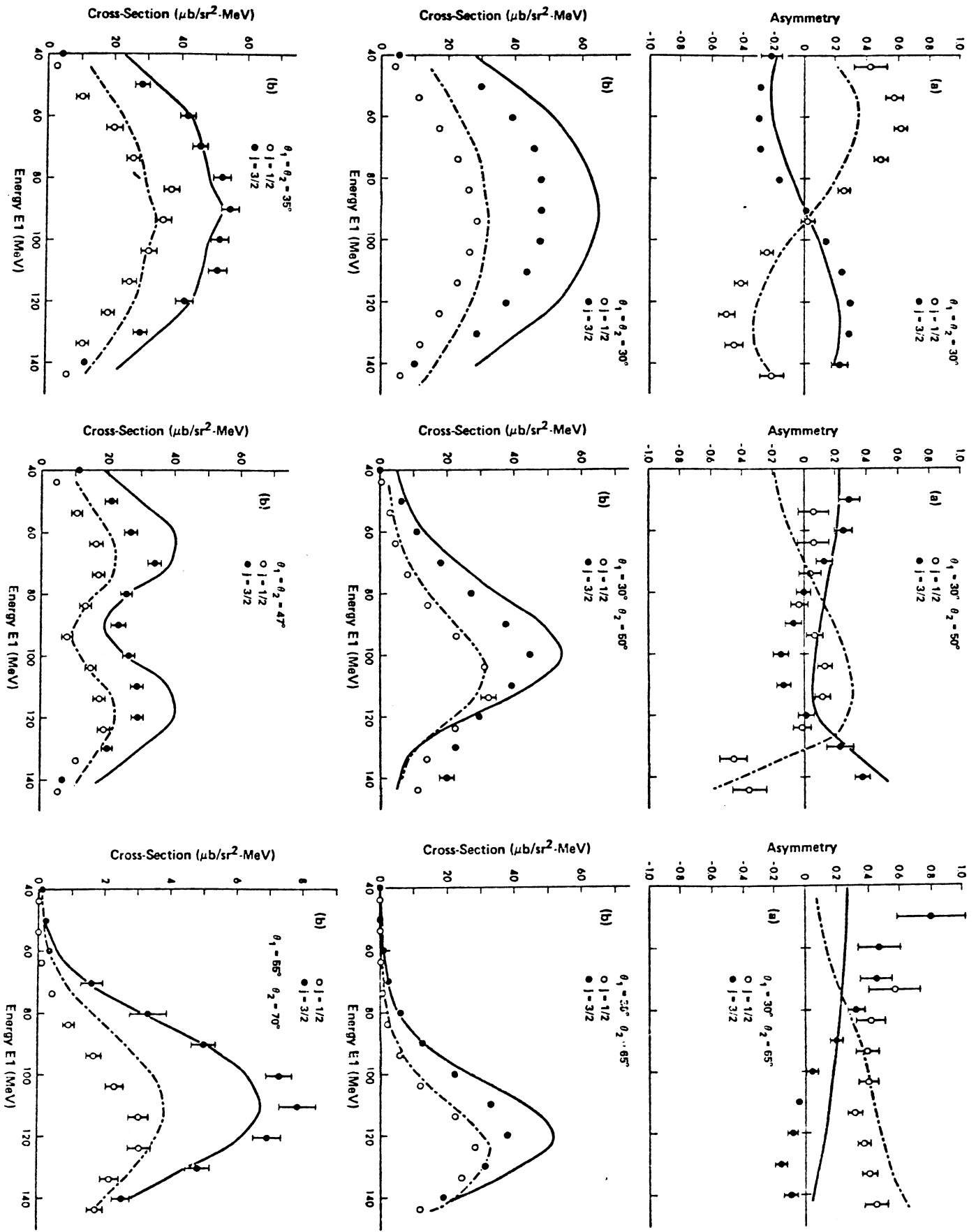


Fig. 28